ARTICLES

Structure of a bacterial multidrug ABC transporter

Roger J. P. Dawson[1] & Kaspar P. Locher[1]

Multidrug transporters of the ABC family facilitate the export of diverse cytotoxic drugs across cell membranes. This is clinically relevant, as tumour cells may become resistant to agents used in chemotherapy. To understand the molecular basis of this process, we have determined the 3.0 Å crystal structure of a bacterial ABC transporter (Sav1866) from *Staphylococcus aureus*. The homodimeric protein consists of 12 transmembrane helices in an arrangement that is consistent with cross-linking studies and electron microscopic imaging of the human multidrug resistance protein MDR1, but critically different from that reported for the bacterial lipid flippase MsbA. The observed, outward-facing conformation reflects the ATP-bound state, with the two nucleotide-binding domains in close contact and the two transmembrane domains forming a central cavity—presumably the drug translocation pathway—that is shielded from the inner leaflet of the lipid bilayer and from the cytoplasm, but exposed to the outer leaflet and the extracellular space.

ATP-binding cassette (ABC) transporters are integral membrane proteins that actively transport chemically diverse substrates across the lipid bilayers of cellular membranes[1]. Clinically relevant examples, including the human proteins MDR1 (also known as ABCB1 or P-glycoprotein) and MRP1 (also known as ABCC1), contribute to multidrug resistance of cancer cells by catalysing the extrusion of cytotoxic compounds used in cancer therapy[2]. Other ABC proteins are associated with various diseases, including cystic fibrosis (mutations in the CFTR protein[3]), or have a central role in the cellular immune system by transporting antigenic peptides (TAP1 and TAP2 proteins[4]). In bacteria, ABC exporters extrude diverse substrates, including drugs and antibiotics, whereas ABC importers mediate the uptake of essential nutrients. One of the best-studied bacterial ABC exporters is the LmrA protein from *Lactobacillus lactis*, which probably contributes to bacterial drug or antibiotic resistance, but in addition has been found to functionally substitute for human MDR1 when expressed in lung fibroblast cells[5].

The basic ABC transporter architecture consists of two transmembrane domains (TMDs) that provide a translocation pathway, and two cytoplasmic, water-exposed nucleotide-binding domains (NBDs) that hydrolyse ATP. Bacterial multidrug ABC proteins are generally expressed as 'half-transporters' that contain one TMD fused to a NBD, which dimerize to form the full transporter. Functionally important residues are highly conserved among the NBDs, suggesting that ABC transporters share a common mechanism of coupling ATP hydrolysis to substrate transport[6,7]. However, despite extensive biochemical, genetic and structural studies, a detailed understanding of the substrate acquisition and transport process has remained elusive. To address these questions, we have determined the crystal structure of *S. aureus* Sav1866, whose primary sequence and biochemical characteristics identify it as a homologue of multidrug ABC transporters. Sav1866 shows significant sequence similarity to human ABC transporters of the subfamily B that includes MDR1 and TAP1/TAP2. Purified Sav1866 is functional in detergent solution as demonstrated by *in vitro* ATPase activity and characteristic inhibition by orthovanadate (Supplementary Fig. S1). When reconstituted in liposomes, its ATPase activity is stimulated by

the cancer drugs doxorubicin and vinblastine, and by the fluorescent dye Hoechst 33342 (Supplementary Fig. S1), all of which are also substrates of *L. lactis* LmrA and human MDR1[8,9].

Sav1866 architecture and domain structure

Our crystallographic analysis yielded electron density of high quality for the entire protein (Supplementary Fig. S2), and the structure was refined to 3.0 Å resolution with good refinement statistics (R_{work} and R_{free} values of 25.5% and 27.2%, respectively). The functional unit of Sav1866 is a dimer of two elongated subunits related by two-fold molecular and non-crystallographic symmetry (Fig. 1a, b). The full transporter is 120 Å long, 65 Å wide and 55 Å deep, and its overall shape is consistent with that of human MDR1 studied at low resolution by electron microscopy[10,11]. Each subunit consists of an amino-terminal TMD (amino-acid residues 1–320) and a carboxy-terminal NBD (residues 337–578). The two subunits exhibit a considerable twist and embrace each other, with both the transmembrane and the nucleotide-binding domains tightly interacting. The polypeptide that links the domains (residues 321–336) emanates from transmembrane (TM) helix TM6 and wraps around the distal side of the NBD (Fig. 1b), similar to the analogous linker observed in the crystal structure of human TAP1[12].

The NBDs of the Sav1866 homodimer are similar in structure to those of other ABC transporters. They expose conserved ATP-binding and -hydrolysis motifs[7] at the shared interface in a 'head-to-tail' arrangement that has been widely accepted as physiologically relevant on the basis of structural[13,14] and biochemical[15–17] data. The hallmark of this arrangement is that two ATP-hydrolysis sites are formed at the shared interface, between the P-loop of one NBD and the ABC signature motif of the other. This creates a direct link between the two sites and provides the molecular basis of the observed cooperativity in ATP binding and hydrolysis[18].

Sav1866 was crystallized in the presence of ADP, and clear electron density was evident for two ADP molecules bound by the P-loops and the ABC signature motifs of opposing subunits. However, the conformation of these motifs is, at the present resolution, indistinguishable from that of isolated nucleotide-binding domains

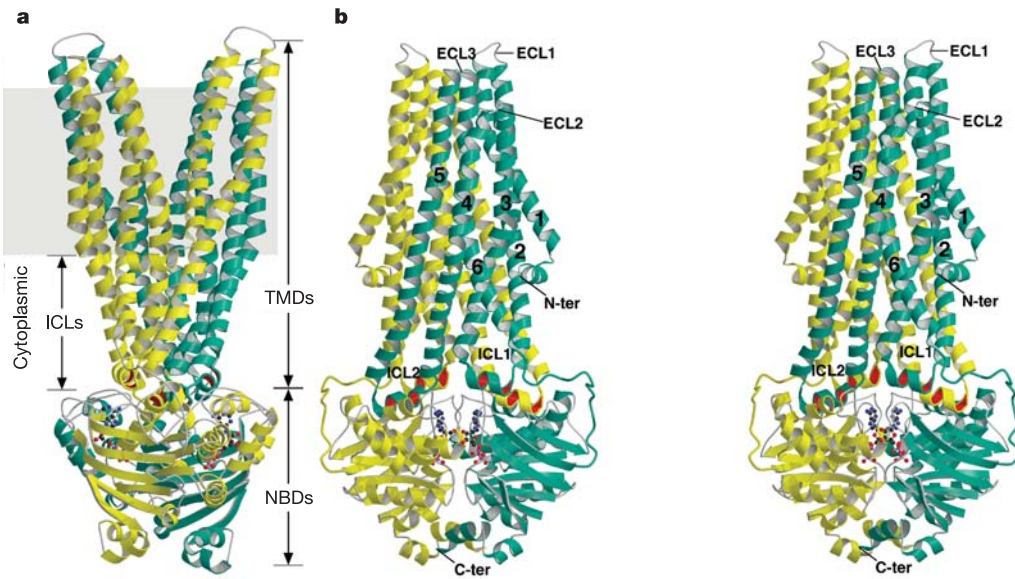[1]Institute of Molecular Biology and Biophysics, ETH Zurich, 8093 Zurich, Switzerland.

Figure 1 | Sav1866 structure. a, Backbone of the homodimeric protein in ribbon representation, with the subunits coloured yellow and turquoise. Bound ADP is in ball-and-stick representation. The view reveals the membrane-embedded 'wings' of the protein; the grey box depicts the probable location of the lipid bilayer on the basis of the hydrophobicity of the protein surface. **b**, Stereo view rotated with respect to **a** by 90° around the

vertical two-fold molecular and non-crystallographic axis. The transmembrane helices of one subunit (turquoise) are numbered. TMDs, transmembrane domains; NBDs nucleotide-binding domains; ICL, intracellular loops (between transmembrane helices); ECL, extracellular loops (between transmembrane helices); N-ter, amino terminus; C-ter, carboxy terminus.

containing trapped ATP (for example, the archaeal ABC protein MJ0796[14]). Specifically, the P-loops and ABC signature motifs tightly sandwich bound nucleotide between them, whereas the structure of the *Escherichia coli* vitamin B_{12} transporter BtuCD, crystallized in the absence of nucleotide[19], revealed a substantial separation of the analogous motifs (Fig. 2). This indicates that although ADP, rather than ATP, was bound, the NBDs in Sav1866 exhibit the conformation of the ATP-bound state. This is consistent with the TMDs adopting an outward-facing conformation (see below). We conclude that our purification and crystallization conditions, in particular the presence of detergent, have shifted the conformational equilibrium of Sav1866 to the ATP-bound state.

Each TMD traverses the lipid bilayer six times to yield 12 transmembrane helices for the homodimeric transporter, in agree-

ment with the canonical ABC exporter topology. Around the middle of the membrane, bundles of transmembrane helices diverge into two discrete 'wings' that point away from one another towards the cell exterior, thus providing an outward-facing conformation. Rather than representing individual TMDs, each 'wing' consists of helices TM1–TM2 from one subunit and TM3–TM6 from the other subunit. The transmembrane segments are connected by long intracellular and short extracellular loops (ICLs and ECLs, respectively). The ICLs extend the helical secondary structure beyond the lipid bilayer and protrude approximately 25 Å into the cytoplasm. Notably, the helices TM1–TM3 are closely related to TM4–TM6 by an approximate two-fold rotation around a symmetry axis parallel to the membrane plane, with a root-mean-square deviation of 5.7 Å for 146 Cα positions (residues 9–154 and 175–320). Rotational symmetry of subsets of
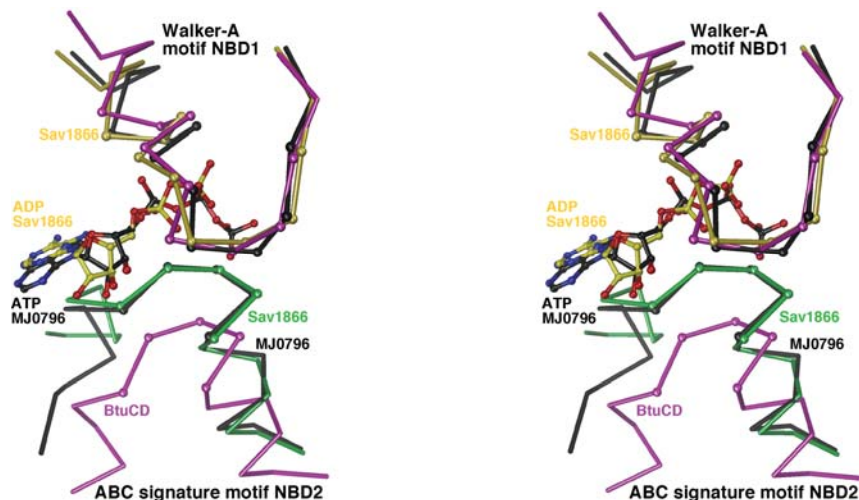

Figure 2 | Superposition of nucleotide-binding domain structures. Both P-loops (Walker-A motifs) of the NBD dimers were used for superposition, but for clarity only one nucleotide-binding site is shown in stereo. The Cα positions of conserved residues GxxGxGKST (P-loop) and LSGGQ (ABC

signature motifs) are depicted as spheres in the backbone traces. Bound nucleotides are in ball-and-stick representation. Note the close superposition of the ABC signature motifs of Sav1866 and MJ0796 compared with that of BtuCD.

transmembrane helices may indicate gene duplication and has been observed in the structures of aquaporins[20] and major facilitators[21], but has not previously been reported for ABC exporters.

The arrangement of transmembrane helices observed for Sav1866 is consistent with recent cross-linking data that identified neighbouring helices in human MDR1[22]. In contrast, the reported X-ray analyses of another ABC exporter, the bacterial lipid flippase MsbA[23–25], show an arrangement distinctly different from the one we describe here (Supplementary Fig. S4 and Supplementary Table S2). With respect to the nucleotide-binding domains, the structure of Sav1866 exhibits close structural agreement with that of MJ0796[14],
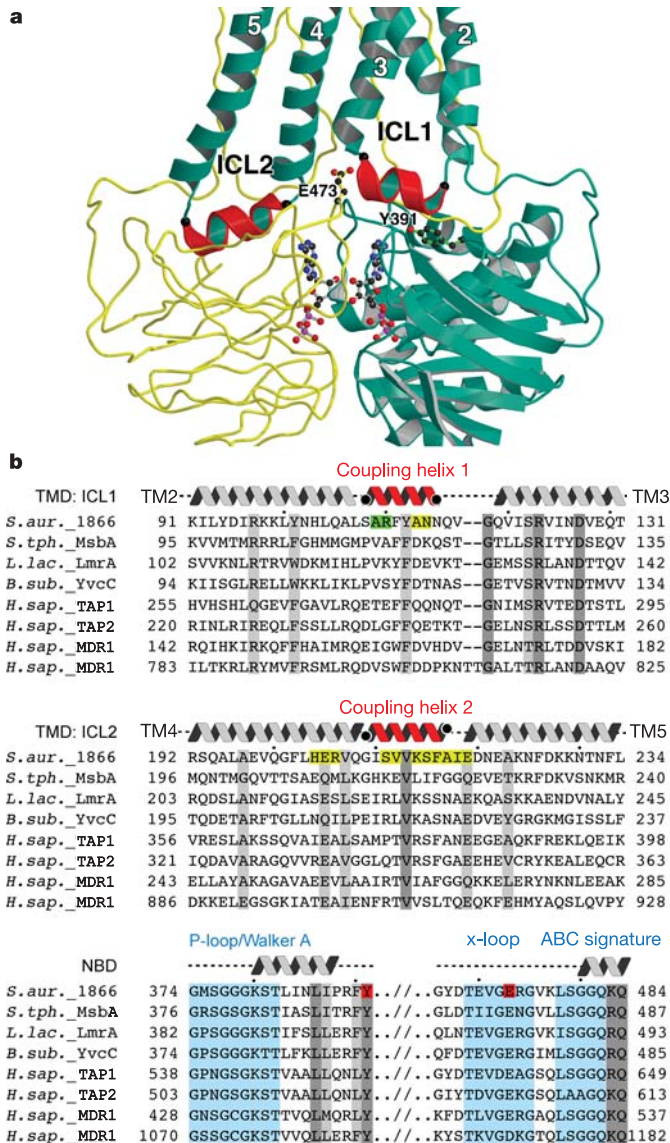
whereas in MsbA of *Salmonella typhimurium*, the analogous domains appear laterally offset and at a greater distance. The observed architectures of MsbA and Sav1866 remain incompatible, even when considering that the proteins may have been trapped in distinct states, and the differences—if real—would indicate a convergent evolution of the two proteins.

Transmission interface

Conformational changes generated by ATP binding and hydrolysis are transmitted from the nucleotide-binding to the transmembrane domains through non-covalent interactions at the shared interface. The TMDs of Sav1866 contribute to this interface mainly through the intracellular loops ICL1 and ICL2. This is consistent with genetic data that implicated ICL1 of human MDR1 to interact with the NBDs[26], and with mutational studies and sequence comparisons that indicated ICL2 of TAP1/TAP2, as well as ICL4 of CFTR, to provide similar crucial contacts[4,27]. In Sav1866, both ICLs contain short helices oriented roughly parallel to the membrane plane and
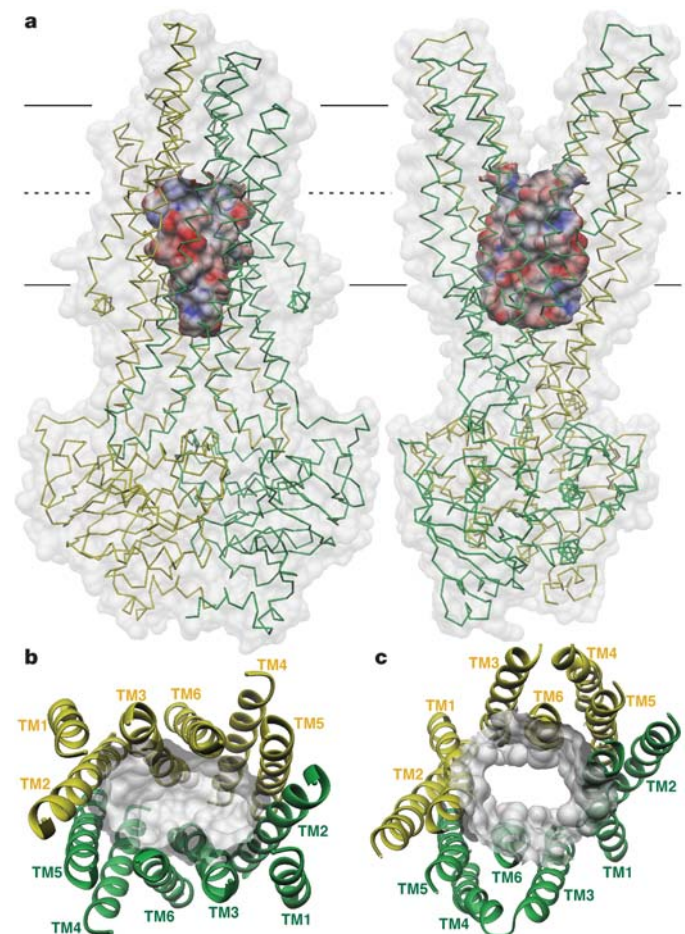

a

b

Coupling helix 1

TMD: ICL1	TM2				TM3
S.aur._1866	91	KILYDIRKKLYNHLQALS	ARFYAN	NQV--GQVISRVINDVEQT	131
S.tph._MsbA	95	KVVMTMRRRLFGHMMGMPVAFFDKQST--GTLLSRITYDSEQV			135
L.lac._LmrA	102	SVVKNLRTRVWDKMIHLPVKYFDEVKT--GEMSSRLANDTTQV			142
B.sub._YvcC	94	KIISGLRELLWKKLIKLPVSYFDTNAS--GETVSRVTNDTMVV			134
H.sap._TAP1	255	HVHSHLQGEVFGAVLRQETEFFQQNQT--GNIMSRVTEDTSTL			295
H.sap._TAP2	220	RINLRIREQLFSSLLRQDLGFFQETKT--GELNSRLSSDTTLM			260
H.sap._MDR1	142	RQIHKIRKQFFHAIMRQEIGWFDVHDV--GELNTRLTDDVSKI			182
H.sap._MDR1	783	ILTKRLRYMVFRSMLRQDVSWFDDPKNTTGALTTRLANDAAQV			825

Coupling helix 2

TMD: ICL2	TM4				TM5
S.aur._1866	192	RSQALAEVQGFL	HERVQGI	SVVKSFAIE	DNEAKNFDKKNTNFL	234
S.tph._MsbA	196	MQNTMGQVTTSAEQMLKGHKEVLIFGGQEVETKRFDKVSNKMR				240
L.lac._LmrA	203	RQDSLANFQGIASESLSEIRLVKSSNAEKQASKKAENDVNALY				245
B.sub._YvcC	195	TQDETARFTGLLNQILPEIRLVKASNAEDVEYGRGKMGISSLF				237
H.sap._TAP1	356	VRESLAKSSQVAIEALSAMPTVRSFANEEGEAQKFREKLQEIK				398
H.sap._TAP2	321	IQDAVARAGQVVREAVGGLQTVRSFGAEEHEVCRYKEALEQCR				363
H.sap._MDR1	243	ELLAYAKAGAVAEEVLAAIRTVIAFGGQKKELERYNKNLEEAK				285
H.sap._MDR1	886	DKKELEGSGKIATEAIENFRTVVSLTQEQKFEHMYAQSLQVPY				928

P-loop/Walker A   x-loop   ABC signature

NBD				
S.aur._1866	374	GMSGGGKSTLINLIPRFY..//..GYDTEVG	E	RGVKLSGGQKQ	484
S.tph._MsbA	376	GRSGSGKSTIASLITRFY..//..GLDTIIGENGVLLSGGQRQ			487
L.lac._LmrA	382	GPSGGGKSTIFSLLERFY..//..QLNTEVGERGVKISGGQRQ			493
B.sub._YvcC	374	GPSGGGKTTLFKLLERFY..//..QFDTEVGERGIMLSGGQRQ			485
H.sap._TAP1	538	GPNGSGKSTVAALLQNLY..//..GYDTEVDEAGSQLSGGQRQ			649
H.sap._TAP2	503	GPNGSGKSTVAALLQNLY..//..GIYTDVGEKGSQLAAGQKQ			613
H.sap._MDR1	428	GNSGCGKSTTVQLMQRLY..//..KFDTLVGERGAQLSGGQKQ			537
H.sap._MDR1	1070	GSSGCGKSTVVQLLERFY..//..KYSTKVGDKGTQLSGGQKQ			1182

Figure 3 | **Transmission interface. a**, Close-up view of Sav1866 with one subunit in turquoise ribbon representation, the other in yellow coil representation. For clarity, only the ICL regions of the transmembrane domains are shown. Black spheres depict the first and last Cα positions of the 'coupling helices' (see the text). Side chains of the conserved Glu 473 and Tyr 391 are in ball-and-stick representation. **b**, Alignment of the Sav1866 protein sequence with those of other ABC transporters. Residues with high conservation are shaded dark grey, those with significant conservation are shaded light grey, and relevant motifs are shaded blue and indicated. Residues of the ICLs interacting (4 Å cut-off) with the NBD of the same subunit are indicated with green shading, and those contacting the opposite NBD with yellow shading. Residues of the NBD interacting with the TMD are shown with red shading.

a

b

c

Figure 4 | **Substrate translocation pathway. a**, Backbone traces of the Sav1866 subunits (green and yellow) in two orientations, rotated by 90° around a vertical axis. The molecular surface of the central cavity is coloured according to its calculated electrostatic potential (blue, positively charged; red, negatively charged), whereas that of the rest of the transporter is in transparent light grey. Lines indicate the approximate position of the two leaflets of the lipid bilayer. Access from the cavity to the outer leaflet of the lipid bilayer is visible in the right panel from the front and back, between the 'wings' formed by the TMDs. **b**, Cavity at the level of the inner leaflet viewed from the extracellular side. The transmembrane helices are numbered and the cavity is shown as a grey surface. **c**, Same as **b** but at the level of the outer leaflet. Note that owing to helix bending, different subsets of helices line the cavity when compared with **b**.

providing the bulk of the contacts (Fig. 3a,b). We refer to these as 'coupling helices' to emphasize their likely involvement in transmitting mechanistically crucial conformational changes. Unexpectedly, the ICLs of Sav1866 reach across and contact primarily the nucleotide-binding domain of the opposite subunit, analogous to domain swapping observed in various enzymes[28]. Although coupling helix 1 contacts the NBDs of both subunits, coupling helix 2 interacts with that of the opposite subunit exclusively. Such swapping has not been anticipated for ABC exporters (Fig. 5), but is not inconsistent with the available biochemical or genetic data. In contrast, the TMDs of the ABC importer BtuCD contact only one NBD, resulting in a large gap at the centre of the four protein domains[19]. The architecture of the ICLs and coupling helices observed in Sav1866 is probably conserved among ABC exporters, as suggested by the significant sequence similarity in the corresponding regions (Fig. 3b).

On the part of the NBDs, the contact surface with the TMD is primarily lined with residues around the so-called 'Q-loop'[7], as was also observed in BtuCD[19]. Two prominent exceptions include the conserved residues Tyr 391 and Glu 473. The latter seems particularly intriguing, as it interacts with both ICLs and is part of a previously unrecognized, short sequence motif (TEVGERG) that appears conserved in ABC export proteins only (Fig. 3b). We refer to this sequence as the 'x-loop' to highlight its apparent function in crosslinking the ICLs. Because the x-loops precede the ABC signature motifs, they probably respond to ATP binding and hydrolysis and may transmit conformational changes to the ICLs by alternating engaging in, and releasing, the cross-link on ATP binding and hydrolysis. The absence of this motif in binding-protein-dependent bacterial ABC importers suggests a distinct coupling mechanism compared with ABC exporters.

Substrate translocation pathway

A large cavity is present at the interface of the two transmembrane domains (Fig. 4). Although shielded from the cytoplasm and the lipid bilayer at the level of the inner leaflet, the cavity is accessible from the outer leaflet and exposed to the extracellular space. The bottom of the cavity reaches beyond the intracellular membrane boundary, but no connection to the cytoplasm exists. At the level of the inner leaflet, the cavity features a hydrophilic surface that is primarily lined with polar and charged amino-acid side chains from helices TM2–TM5, with a slight surplus of negative charges and no significant hydrophobic patches. At the level of the outer leaflet, the translocation pathway is lined with residues from helices TM1, TM3 and TM6.

The observed cavity is consistent with an outward-facing conformation of the ATP-bound state of human MDR1, as revealed by electron microscopy[10,29]. The predominance of polar and charged

amino acids suggests that rather than a high-affinity binding site, the observed cavity in Sav1866 may reflect an extrusion pathway with little or no affinity for hydrophobic drugs. Binding of substrates to human MDR1 was indeed significantly reduced in the presence of ATP[30]. Similarly, LmrA exposes a high-affinity binding site to the interior of the cell, whereas in the ATP-bound state, this site is occluded and a weak binding site is accessible from the extracellular space[9].

The architecture of Sav1866 indicates that residues from all transmembrane helices contribute to the surface of the translocation pathway. It was noted recently that, despite extensive efforts, no well-defined substrate binding sites have been identified in ABC exporters[31]. Residues from transmembrane helices TM1, TM4–TM6 and TM10–TM12 have been implicated in drug binding to human MDR1[32], whereas residues from multiple helices have been found to contribute to substrate binding to TAP1/TAP2[33]. The analogous residues in Sav1866 indeed point towards the translocation pathway.

Transport mechanism

The simplest scheme of the transport mechanism invokes two states: an inward-facing conformation with the substrate binding site accessible from the cell interior, and an outward-facing conformation with an extrusion pocket exposed to the external medium. The structure of Sav1866 reveals that tight interaction of the NBDs in the ATP-bound state is coupled to the outward-facing conformation of the TMDs. In this conformation, bound substrates may escape into the outer leaflet of the lipid bilayer or into the aqueous medium surrounding the cell, depending on their hydrophobicity. Hydrolysis of ATP is expected to return the transporter to an inward-facing conformation, again granting access to the binding site from the cell interior. ABC transporters may thus use an "alternating access and release" mechanism first postulated for major facilitator transport proteins[34], with the distinction that ATP binding and hydrolysis, rather than substrate acquisition, may control the conversion of one state into the other. Most ABC transporters bind and hydrolyse two ATP molecules in each reaction cycle[35,36]. However, the number of bound substrates can vary, and—depending on the molecular mass— up to two substrates have been found to enter the binding pockets of human MDR1 and MRP2[37,38]. We conclude that if two small substrates are bound, the apparent stoichiometry of hydrolysed ATP per transported substrate will be one, whereas for a single, larger substrate, it will be two.

The architecture of the TMD–NBD interface of Sav1866 defies the widely used ABC exporter schematic shown in Fig. 5a. Rather than aligned side-by-side, the two subunits of Sav1866 are intricately associated (Fig. 5b) and the main interface of the intracellular loops is with the NBD of the opposite subunit. Furthermore, helices from both TMDs form the two 'wings' consisting of bundles of helices embedded in the membrane (Fig. 1a). Given these constraints, the two subunits are unlikely to move independently and their maximum separation during the reaction cycle is therefore limited. Our results challenge mechanistic models that suggest that NBDs dimerize on binding ATP and dissociate on completing a transport cycle[31,39,40]. Although this is true for purified, isolated NBDs, electron microscopic studies of full-length MDR1 and CFTR have demonstrated close proximity of the NBDs in the absence of nucleotide[11,41], as has the crystallographic analysis of BtuCD[19].

Compared with Sav1866, the ABC signature motifs of the nucleotide-free state of BtuCD are separated by an additional ~5 Å from the P-loops (Fig. 2), a conformational rearrangement that reduces the interface between opposing NBDs. Solvent accessibility of the nucleotide-binding site in the bacterial maltose transporter is indeed decreased in the absence of ATP[42], as is the energetic coupling between side chains at the NBD interface of CFTR[17]. The 'power stroke' of ABC transporters, triggered by binding of ATP, may thus consist of moderate conformational rearrangements that originate at the interface of the two NBDs and propagate towards the TMDs.

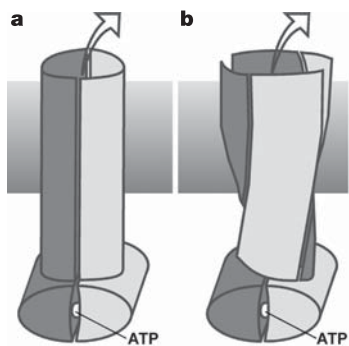In addition to its value for investigating the drug extrusion

Figure 5 | ABC exporter schematics. a, Earlier cartoons depict two compact transporter halves (subunits) arranged side-by-side, suggesting separation during the transport cycle. The grey box indicates the location of the membrane. **b,** Schematic of Sav1866 in the observed, outward-facing conformation. The cartoon emphasizes the domain swapping and subunit twisting. Arrows indicate the release of bound drug into the extracellular space.

mechanism, the Sav1866 structure may be useful for interpreting mutations of human ABC transporters of known substrates or proven implication in disease. A notable example is the deletion-mutation Δ508 (a Phe residue) of CFTR, responsible for 70% of cystic fibrosis cases[43,44]. The analogous residue in Sav1866 is revealed as Leu 437 by superposition with the NBD of wild-type and Δ508-mutant CFTR[45]. Leu 437 is part of a cluster of aromatic and hydrophobic side chains at the interface of ICL2 and the NBD. Given this structural context, the absence of the Phe side chain in CFTR Δ508, despite limited impact on the protein backbone, probably destabilizes the analogous packing of residues at the interface of NBD1 and ICL4, thus contributing to the observed misassembly of the mutant CFTR protein.

Conclusions

Our results define, at high resolution, the architecture of a bacterial multidrug ABC transporter in the outward-facing conformation, with a single substrate translocation pathway exposed to the extra-cellular environment. Because the structure of Sav1866 agrees well with genetic, biochemical and structural data of bacterial and human homologues, it most likely reflects a physiologically relevant state. It visualizes the arrangement of the canonical 12 transmembrane helices forming the core of ABC exporter proteins. Given that high-resolution structures of clinically relevant ABC transporters are currently not available, Sav1866 may serve as a valuable structural model of human homologues and may initiate the rational design of drugs aimed at interfering with the extrusion of agents used in chemotherapy. The challenge for future studies will be to trap and visualize the transporter in the inward-facing conformation that allows substrates to access the high-affinity binding site.

METHODS

Sav1866 was selected from a pool of bacterial ABC exporter homologues on the basis of its superior biochemical stability and its ability to form well-ordered, three-dimensional crystals. The gene encoding Sav1866 was cloned from *S. aureus* genomic DNA by polymerase chain reaction (PCR) and fused to an N-terminal decahistidine affinity tag in a modified T7 expression vector. The transporter was overexpressed in *E. coli*, solubilized from isolated cell membranes, and purified in octaethylene glycol monododecyl ether ($C_{12}E_8$) as a detergent. Protein crystals were obtained by vapour diffusion and belonged to the space group *C*2 with one full transporter per asymmetric unit. Diffraction data were collected at the beamline X06SA of the Swiss Light Source (SLS). The structure was phased by multiple isomorphous replacement with anomalous scattering using data from various derivative crystals (Supplementary Table S1). Excellent experimental density was visible for the entire molecule, including loops connecting transmembrane helices (Supplementary Fig. S2), and model build-ing was further aided by the presence of selenomethionines serving as marker positions (Supplementary Fig. S3). Except for extracellular loops engaged in lattice contacts, and a few residues with distinct side-chain conformations at the subunit interface, no differences are visible between the two non-crystal-lographically related subunits. Details of the biochemical and crystallographic procedures are given in Supplementary Information. Figures 1 and 2 were prepared using MolScript (http://www.avatar.se/molscript) and Raster3D (http://skuld.bmsc.washington.edu/raster3d), Figs 3 and 4 using DINO (http://www.dino3d.org) and MSMS (http://www.scripps.edu/~sanner/html/msms_home.html). Electrostatic potentials were calculated using MEAD (http://www.scripps.edu/mb/bashford).

1. Holland, I. B., Cole, S. P. C., Kuchler, K. & Higgins, C. F. *ABC Proteins: From Bacteria to Man* (Academic, London, 2003).
2. Gottesman, M. M. & Ambudkar, S. V. Overview: ABC transporters and human disease. *J. Bioenerg. Biomembr.* **33**, 453–458 (2001).
3. Sheppard, D. N. & Welsh, M. J. Structure and function of the CFTR chloride channel. *Physiol. Rev.* **79**, S23–S45 (1999).
4. Lankat-Buttgereit, B. & Tampe, R. The transporter associated with antigen processing: function and implications in human diseases. *Physiol. Rev.* **82**, 187–204 (2002).
5. van Veen, H. W. *et al.* A bacterial antibiotic-resistance gene that complements the human multidrug-resistance P-glycoprotein gene. *Nature* **391**, 291–295 (1998).
6. Holland, I. B. & Blight, M. A. ABC-ATPases, adaptable energy generators fuelling transmembrane movement of a variety of molecules in organisms from bacteria to humans. *J. Mol. Biol.* **293**, 381–399 (1999).
7. Schneider, E. & Hunke, S. ATP-binding-cassette (ABC) transport systems: functional and structural aspects of the ATP-hydrolyzing subunits/domains. *FEMS Microbiol. Rev.* **22**, 1–20 (1998).
8. Shapiro, A. B. & Ling, V. Reconstitution of drug transport by purified P-glycoprotein. *J. Biol. Chem.* **270**, 16167–16175 (1995).
9. van Veen, H. W., Margolles, A., Muller, M., Higgins, C. F. & Konings, W. N. The homodimeric ATP-binding cassette transporter LmrA mediates multidrug transport by an alternating two-site (two-cylinder engine) mechanism. *EMBO J.* **19**, 2503–2514 (2000).
10. Rosenberg, M. F., Callaghan, R., Modok, S., Higgins, C. F. & Ford, R. C. Three-dimensional structure of P-glycoprotein—the transmembrane regions adopt an asymmetric configuration in the nucleotide-bound state. *J. Biol. Chem.* **280**, 2857–2862 (2005).
11. Lee, J. Y., Urbatsch, I. L., Senior, A. E. & Wilkens, S. Projection structure of P-glycoprotein by electron microscopy—evidence for a closed conformation of the nucleotide binding domains. *J. Biol. Chem.* **277**, 40125–40131 (2002).
12. Gaudet, R. & Wiley, D. C. Structure of the ABC ATPase domain of human TAP1, the transporter associated with antigen processing. *EMBO J.* **20**, 4964–4972 (2001).
13. Hopfner, K. P. *et al.* Structural biology of Rad50 ATPase: ATP-driven conformational control in DNA double-strand break repair and the ABC-ATPase superfamily. *Cell* **101**, 789–800 (2000).
14. Smith, P. C. *et al.* ATP binding to the motor domain from an ABC transporter drives formation of a nucleotide sandwich dimer. *Mol. Cell* **10**, 139–149 (2002).
15. Hrycyna, C. A. *et al.* Mechanism of action of human P-glycoprotein ATPase activity—photochemical cleavage during a catalytic transition state using orthovanadate reveals cross-talk between the two ATP sites. *J. Biol. Chem.* **273**, 16631–16634 (1998).
16. Chen, J., Sharma, S., Quiocho, F. A. & Davidson, A. L. Trapping the transition state of an ATP-binding cassette transporter: evidence for a concerted mechanism of maltose transport. *Proc. Natl Acad. Sci. USA* **98**, 1525–1530 (2001).
17. Vergani, P., Lockless, S. W., Nairn, A. C. & Gadsby, D. C. CFTR channel opening by ATP-driven tight dimerization of its nucleotide-binding domains. *Nature* **433**, 876–880 (2005).
18. Senior, A. E. & Bhagat, S. P-glycoprotein shows strong catalytic cooperativity between the two nucleotide sites. *Biochemistry* **37**, 831–836 (1998).
19. Locher, K. P., Lee, A. T. & Rees, D. C. The *E. coli* BtuCD structure: a framework for ABC transporter architecture and mechanism. *Science* **296**, 1091–1098 (2002).
20. Stroud, R. M. *et al.* Glycerol facilitator GlpF and the associated aquaporin family of channels. *Curr. Opin. Struct. Biol.* **13**, 424–431 (2003).
21. Abramson, J., Kaback, H. R. & Iwata, S. Structural comparison of lactose permease and the glycerol-3-phosphate antiporter: members of the major facilitator superfamily. *Curr. Opin. Struct. Biol.* **14**, 413–419 (2004).
22. Stenham, D. R. *et al.* An atomic detail model for the human ATP binding cassette transporter P-glycoprotein derived from disulphide cross-linking and homology modeling. *FASEB J.* **17**, 2287–2289 (2003).
23. Chang, G. & Roth, C. B. Structure of MsbA from *E. coli*: a homolog of the multidrug resistance ATP binding cassette (ABC) transporters. *Science* **293**, 1793–1800 (2001).
24. Chang, G. Structure of MsbA from *Vibrio cholera*: a multidrug resistance ABC transporter homolog in a closed conformation. *J. Mol. Biol.* **330**, 419–430 (2003).
25. Reyes, C. L. & Chang, G. Structure of the ABC transporter MsbA in complex with ADP-vanadate and lipopolysaccharide. *Science* **308**, 1028–1031 (2005).
26. Currier, S. J. *et al.* Identification of residues in the first cytoplasmic loop of P-glycoprotein involved in the function of chimeric human MDR1–MDR2 transporters. *J. Biol. Chem.* **267**, 25153–25159 (1992).
27. Cotten, J. F., Ostedgaard, L. S., Carson, M. R. & Welsh, M. J. Effect of cystic fibrosis-associated mutations in the fourth intracellular loop of cystic fibrosis transmembrane conductance regulator. *J. Biol. Chem.* **271**, 21279–21284 (1996).
28. Liu, Y. & Eisenberg, D. 3D domain swapping: as domains continue to swap. *Protein Sci.* **11**, 1285–1299 (2002).
29. Rosenberg, M. F. *et al.* Repacking of the transmembrane domains of P-glycoprotein during the transport ATPase cycle. *EMBO J.* **20**, 5615–5625 (2001).
30. Ramachandra, M. *et al.* Human P-glycoprotein exhibits reduced affinity for substrates during a catalytic transition state. *Biochemistry* **37**, 5010–5019 (1998).
31. Higgins, C. F. & Linton, K. J. The ATP switch model for ABC transporters. *Nature Struct. Mol. Biol.* **11**, 918–926 (2004).
32. Loo, T. W. & Clarke, D. M. Recent progress in understanding the mechanism of P-glycoprotein-mediated drug efflux. *J. Membr. Biol.* **206**, 173–185 (2005).
33. Nijenhuis, M. & Hammerling, G. J. Multiple regions of the transporter associated with antigen processing (TAP) contribute to its peptide binding site. *J. Immunol.* **157**, 5467–5477 (1996).
34. Jardetzky, O. Simple allosteric model for membrane pumps. *Nature* **211**, 969–970 (1966).

35. Patzlaff, J. S., van der Heide, T. & Poolman, B. The ATP/substrate stoichiometry of the ATP-binding cassette (ABC) transporter OpuA. *J. Biol. Chem.* **278,** 29546–29551 (2003).

36. Sauna, Z. E. & Ambudkar, S. V. Evidence for a requirement for ATP hydrolysis at two distinct steps during a single turnover of the catalytic cycle of human P-glycoprotein. *Proc. Natl Acad. Sci. USA* **97,** 2515–2520 (2000).

37. Shapiro, A. B. & Ling, V. Positively cooperative sites for drug transport by P-glycoprotein with distinct drug specificities. *Eur. J. Biochem.* **250,** 130–137 (1997).

38. Zelcer, N. *et al.* Evidence for two interacting ligand binding sites in human multidrug resistance protein 2 (ATP binding cassette C2). *J. Biol. Chem.* **278,** 23538–23544 (2003).

39. Moody, J. E., Millen, L., Binns, D., Hunt, J. F. & Thomas, P. J. Cooperative, ATP-dependent association of the nucleotide binding cassettes during the catalytic cycle of ATP-binding cassette transporters. *J. Biol. Chem.* **277,** 21111–21114 (2002).

40. Chen, J., Lu, G., Lin, J., Davidson, A. L. & Quiocho, F. A. A tweezers-like motion of the ATP-binding cassette dimer in an ABC transport cycle. *Mol. Cell* **12,** 651–661 (2003).

41. Awayn, N. H. *et al.* Crystallographic and single-particle analyses of native and nucleotide-bound forms of the cystic fibrosis transmembrane conductance regulator (CFTR) protein. *Biochem. Soc. Trans.* **33,** 996–999 (2005).

42. Mannering, D. E., Sharma, S. & Davidson, A. L. Demonstration of conformational changes associated with activation of the maltose transport complex. *J. Biol. Chem.* **276,** 12362–12368 (2001).

43. Kerem, B. S. *et al.* Identification of mutations in regions corresponding to the two putative nucleotide (ATP)-binding folds of the cystic-fibrosis gene. *Proc. Natl Acad. Sci. USA* **87,** 8447–8451 (1990).

44. Tsui, L. C. The spectrum of cystic-fibrosis mutations. *Trends Genet.* **8,** 392–398 (1992).

45. Lewis, H. A. *et al.* Impact of the ΔF508 mutation in first nucleotide-binding domain of human cystic fibrosis transmembrane conductance regulator on domain folding and structure. *J. Biol. Chem.* **280,** 1346–1353 (2005).